Mischungsenthalpien beim flüssigen System Wasser + Essigsäure

R. HAASE, P. STEINMETZ und K.-H. DÜCKER

Lehrstuhl für Physikalische Chemie II
der Rheinisch-Westfälischen Technischen Hochschule Aachen

(Z. Naturforsch. **27 a**, 1527—1529 [1972]; eingeg. am 14. August 1972)

Heats of Mixing for the Liquid System Water + Acetic Acid

Calorimetric measurements of the heats of mixing for the liquid system water + acetic acid at 17 °C, 20 °C, 25 °C, 30 °C, 40 °C, and 50 °C show that there is a change of sign in the function $\overline{H}^E(x)$, where $\overline{H}^E$ denotes the molar heat of mixing and x the mole fraction of acetic acid. The process of mixing the pure liquid components is weakly exothermic for low acid concentrations, but strongly endothermic for high acid concentrations. The function $\overline{H}^E$ can be approximately represented by the usual power series with respect to x, five free parameters at each temperature being necessary.

Für das flüssige System Wasser + Essigsäure gibt es nur wenige Daten, die das thermodynamische Verhalten im gesamten Mischungsbereich erfassen. Insbesondere über die Mischungsenthalpie liegen, soweit uns bekannt, lediglich die Messungen von FAUCON [1] bzw. SANDONNINI [2] vor, die aus dem Jahre 1910 bzw. 1913 stammen und sich auf eine Temperatur von 17 °C bzw. auf einen Temperaturbereich von 16 °C bis 18 °C beziehen.

Wir haben deshalb die molare Zusatzenthalpie $\overline{H}^E$ (molare Mischungsenthalpie, molare Mischungswärme) im gesamten Konzentrationsgebiet (mit Ausnahme der Gebiete sehr hoher und sehr niedriger Säurekonzentrationen) bei sechs verschiedenen Temperaturen zwischen 17 °C und 50 °C kalorimetrisch ermittelt.

Die Kalorimetrie ist in einer Apparatur durchgeführt worden, die eine Verbesserung des von GROSSE-WORTMANN [3] beschriebenen Kalorimeters darstellt. Einzelheiten müssen an anderer Stelle nachgelesen werden [4].

Tab. 1. Werte der freien Parameter in Gl. (1) bei verschiedenen Werten der Celsius-Temperatur ϑ.

ϑ / °C	a / J mol^{-1}	b / J mol^{-1}	c / J mol^{-1}	d / J mol^{-1}	e / J mol^{-1}
17	1257,9	851,2	291,4	938,9	−1180,9
20	1278,9	961,2	12,7	730,9	− 732,7
25	1198,4	1298,0	325,9	−28,9	−1341,9
30	1392,4	723,4	13,4	1170,9	− 234,1
40	1440,3	721,2	361,0	930,7	− 506,2
50	1534,8	611,0	96,2	1051,2	291,0

Da im hier interessierenden Konzentrationsbereich die Dissoziation der Essigsäure praktisch vernachlässigbar ist, kann das System Wasser + Essigsäure wie eine binäre Nichtelektrolytlösung behandelt werden. Wir schreiben daher für gegebene Temperatur und gegebenen Druck in bekannter Weise die Größe $\overline{H}^E$ als Potenzreihe im Molenbruch x der Essigsäure:

$$\overline{H}^E = x(1-x) \cdot [a + b(2x-1) + c(2x-1)^2 + d(2x-1)^3 + e(2x-1)^4]. \quad (1)$$

Dabei begnügen wir uns mit den fünf freien Parametern $a, \ldots, e$, die von der Temperatur und (geringfügig) vom Druck abhängen. (Der Druck ist bei unseren Messungen praktisch stets Atmosphärendruck.)

In Abb. 1 bis Abb. 6 sind die bei den sechs Meßtemperaturen experimentell gewonnenen Werte der Funktion $\overline{H}^E(x)$ den nach Gl. (1) mit den Parametern in Tab. 1 berechneten Werten gegenübergestellt. Die gewählte fünfparametrige Darstellung gibt zwar keine

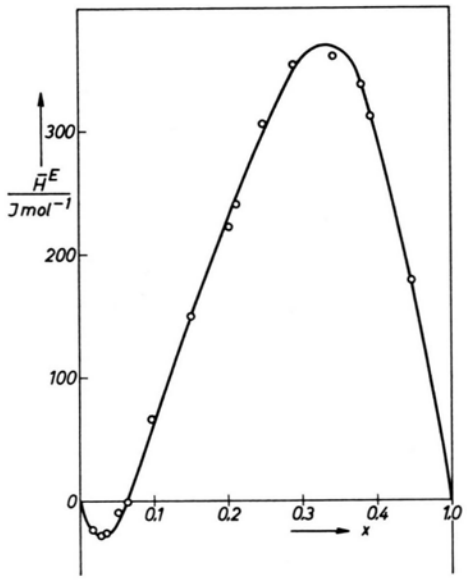

Abb. 1. Gemessene (○) und nach Gl. (1) berechnete (——) Werte der molaren Zusatzenthalpie $\overline{H}^E$ in Abhängigkeit vom Molenbruch x der Essigsäure bei 25 °C.

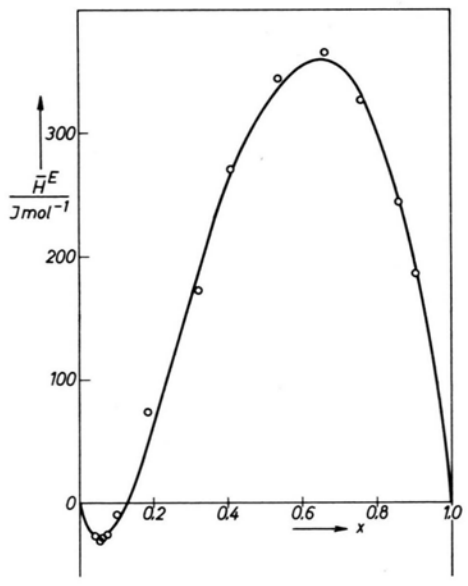

Abb. 2. Funktion $\overline{H}^E(x)$ bei 20 °C.

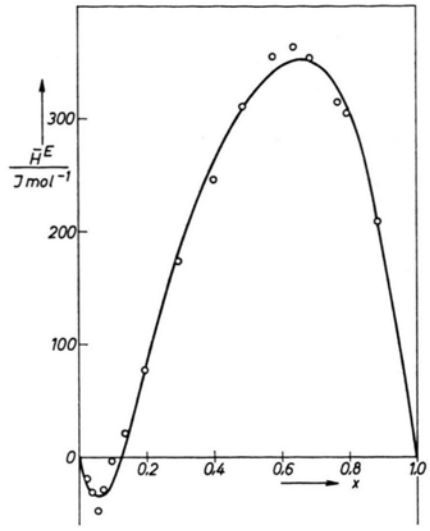

Abb. 3. Funktion $\overline{H}^{E}(x)$ bei 17 °C.

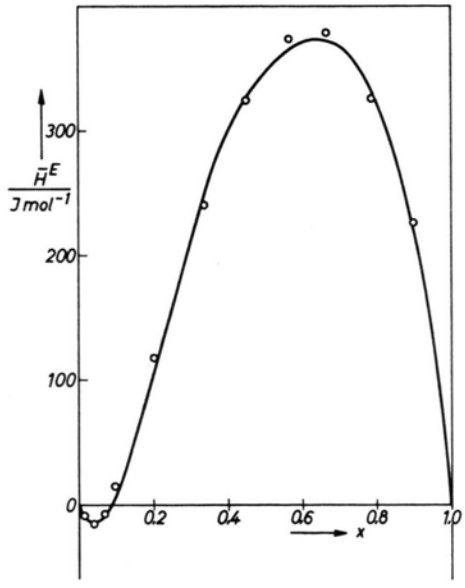

Abb. 4. Funktion $\overline{H}^{E}(x)$ bei 30 °C.

Tab. 2. Gemessene Werte der molaren Zusatzenthalpie $\overline{H}^{E}$ in Abhängigkeit vom Molenbruch x der Essigsäure bei 25 °C.

x	$\overline{H}^{E}$ / J mol^{-1}	x	$\overline{H}^{E}$ / J mol^{-1}
0,0347	−22,88	0,4233	240,64
0,0555	−28,67	0,4980	306,14
0,0698	−26,22	0,5823	354,13
0,1067	− 9,88	0,6876	361,21
0,1281	− 2,59	0,7636	336,92
0,1984	66,46	0,7910	312,02
0,3047	150,43	0,8949	179,28
0,4058	222,28		

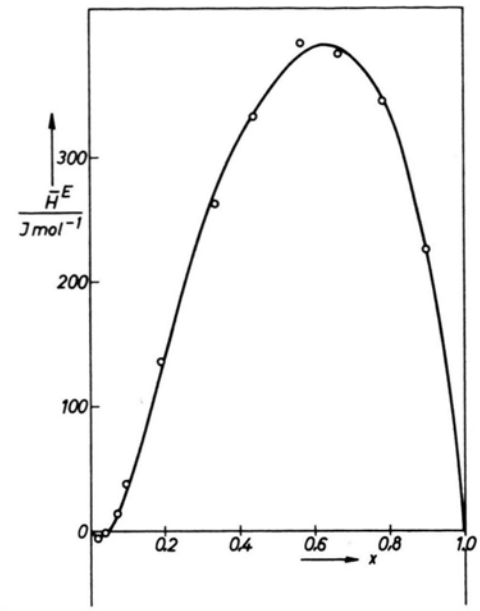

Abb. 5. Funktion $\overline{H}^{E}(x)$ bei 40 °C.

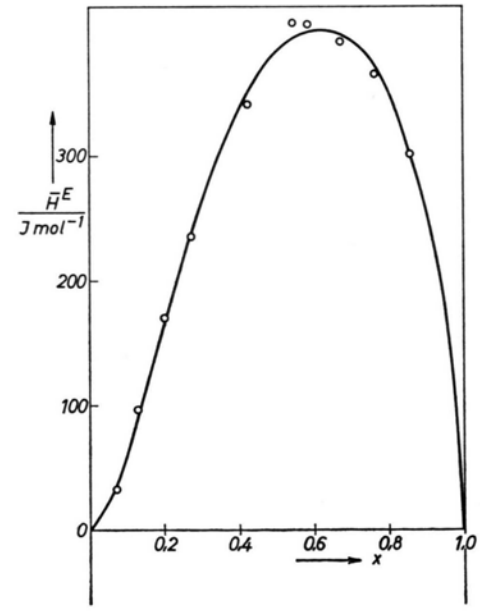

Abb. 6. Funktion $\overline{H}^{E}(x)$ bei 50 °C.

quantitative Übereinstimmung, ist aber qualitativ korrekt. In Tab. 2 sind die Meßwerte für $\overline{H}^{E}$ bei 25 °C zur genaueren Information nochmals zusammengestellt.

Das auffallendste Ergebnis ist der Vorzeichenwechsel von $\overline{H}^{E}$ in dem Sinne, daß der Mischungsvorgang (Bildung der flüssigen Mischung aus den reinen flüssigen Komponenten) bei kleinen Säurekonzentrationen schwach exotherm, bei großen Säurekonzentrationen aber stark

endotherm verläuft. Dabei wird der Bereich des exothermen Mischens ($\overline{H}^E < 0$) mit zunehmender Temperatur immer kleiner.

Bei Vergleich mit den älteren Daten [1, 2] ergibt sich gute Übereinstimmung im Konzentrationsintervall $0 < x < 0{,}6$.

Kalorimetrische Daten aus der Literatur [1, 2, 5] über flüssige Systeme des Typs Wasser + Monocarbonsäure zeigen, daß H^E für Wasser + Ameisensäure stets negativ, für Wasser + Propionsäure und Wasser + Buttersäure aber immer positiv ist. Das System Wasser + Essigsäure nimmt also eine Zwischenstellung ein.

[1] M. A. FAUCON, Ann. Chim. Phys. **8**, 19, 70 [1910].
[2] C. SANDONNINI, Atti Accad. Lincei **22**, 1, 20 [1913].
[3] H. GROSSE-WORTMANN, Dissertation, Universität Göttingen 1964.
[4] P. STEINMETZ, Dissertation, Rheinisch-Westfälische Technische Hochschule Aachen 1972.
[5] A. N. CAMPBELL, J. Amer. Chem. Soc. **59**, 2, 2481 [1937].

Kinetics of Ester-interchange between Methyl Acetate and Ethanol

T. S. RAO and B. R. GANDHE

Department of Chemistry, University of Poona
Poona-7 (India)

(Z. Naturforsch. **27 a**, 1529—1530 [1972]; received 10 August 1972)

Kinetics of ester-interchange between methyl acetate and ethanol has been studied in the range 80—105°, using gas chromatographic technique. The reaction is of the second order, and the specific reaction rate is $29.6 \cdot 10^{-8}$ l/mole-sec at 105°. The energy of activation is 16.7 kcal/mole and the entropy of activation is −44.3 cal/mole-deg.

Ester-interchange is usually a very slow reaction, catalysed either by acid or base [1] and a study of its kinetics is often tedious because of the difficulty of quantitative estimation of low concentrations of the products. Hence it is not surprising that kinetic data on ester-interchange are scarce [2, 3]. The high resolving power and extreme sensitivity of gas chromatography enable minute amounts of reaction products to be estimated, so that the kinetics of even very slow reactions can be studied [4–6]. Hence the technique has been adopted to study the kinetics of a typical ester-interchange, namely the one between methyl acetate and ethanol, catalysed by sodium carbonate, the products being ethyl acetate and methanol.

In each of several Pyrex test tubes 4 ml of an equimolar mixture of methyl acetate and ethanol and 2 g of anhydrous sodium carbonate (80 − 100 mesh) were placed. The tubes were sealed off and placed in a thermostat at 80°. After known intervals of time one tube at a time was withdrawn, cooled rapidly to room temperature, and cut open. The reaction mixture was filtered and analysed using a Beckman Gas Chromatograph GC-2. Nitrogen was the carrier gas at an inlet pressure of 2 kg/cm² and a flow rate of 40 ml/min. The column was a copper tube (2 m long, 6 mm i. d.) packed with Celite (40 − 60 mesh), loaded with 20% Carbowax 4000. The detector was a thermal conductivity cell with a filament current of 150 mA. The temperature of the column and the detector was 70°. The chromatograms were recorded on Bristol Dynamaster Recorder with a sensitivity of 1 mV for full scale deflection.

Each time 5 μl of the reaction mixture were injected into the GC column and the peaks of the products were recorded. These peaks were evaluated from a calibration curve obtained by recording the peaks for different volumes of an equimolar mixture of ethyl acetate and methanol.

If y μl of the products were formed after a given time, their concentration (x) was given by

$$x = (y/5)/0.1382 \text{ moles/l},$$

since the volume of a mixture of a mole each of ethyl acetate and methanol was 138.2 ml, and 5 μl of the reaction mixture were injected into the column. Further, in an equimolar mixture of the reactants the concentration (a) of each was $a = 7.26$ moles/l, since 137.8 ml was the volume of a mixture of a mole each of methyl acetate and ethanol. A plot of $(1/a - x)$ versus time was linear (Fig. 1) implying that the reaction was of the second order. The slope of the plot was the specific reaction rate (k).

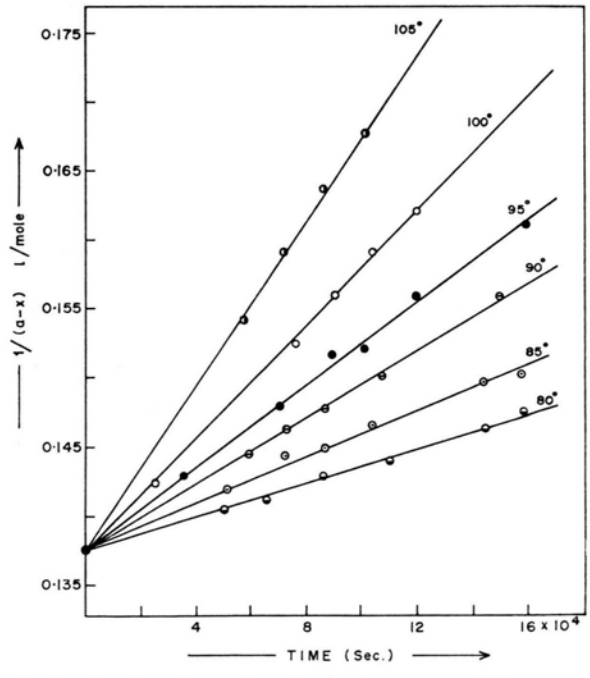

Fig. 1. Kinetics of ester-interchange between methyl acetate and ethanol.

Table 1. Kinetics of ester-interchange between methyl acetate and ethanol. Vairation of specific reaction rate (k) with temperature.

Temperature (°C)	80	85	90	95	100	105
Specific reaction rate k (10^{-8} l/mole-sec)	5.91	8.62	12.3	15.0	21.1	29.6

The experiment was repeated at several temperatures in the range 80 – 105° (Ref. Table 1).

From the results the energy of activation was evaluated to be 16.7 kcal/mole and the entropy of activation to be −44.3 cal/deg. mole.

Thanks are due to Prof. H. J. ARNIKAR, Senior Professor and Head of the Department of Chemistry, University of Poona, for the facilities provided. Further, one of us (B.R.G.) is grateful to the U.G.C. New Delhi, for the award of a Junior Research Fellowship.

[1] J. D. ROBERTS and M. C. CASERIO, Basic Principles of Organic Chemistry, W. A. Benjamin, Inc., New York 1965, p. 532.
[2] A. N. PUDOVIK, R. A. CHERKASOV, and R. M. KONDRATEVA, Vysokomol. Soedin, Ser. A **9** (5), 1118 [1967].
[3] J. HRIVNAK, Z. VESELA, E. SOHLER, and J. DRUBEK, Chem. Prumysl. **15** (1), 7 [1965].
[4] H. J. ARNIKAR, T. S. RAO, and A. A. BODHE, J. Chromatog. **47**, 265 [1970].
[5] P. LORRAINE, P. ROWLAND, MACK, H. CHARLES, COLL, and E. EMERY, J. Gas Chromatog. **6** (3), 173 [1968].
[6] V. PETERKA, ZBIROVSKY, and MIROSLAV, Collect. Czech. Chem. Commun. **35** (3), 1010 [1970].

Excitation of N_2^+ by Vibrating Nitrogen Molecules

R. J. ALDERSON * and B. BROCKLEHURST **

Chemistry Department, Sheffield University, U.K.

(Z. Naturforsch. **27 a**, 1530—1532 [1972]; received 2 September 1972)

Flowing nitrogen gas, bombarded by 50 keV electrons, emits the first negative and second positive bands. Operation of a microwave discharge upstream enhances the former, but not the latter: this is shown to be due to conversion of vibrational excitation in N_2 into electronic excitation in N_2^+.

OLDENBERG [1] has reviewed excitation processes in nitrogen discharges and afterglows. The $B \rightarrow X$, first negative bands of N_2^+ are directly excited from N_2 in the negative glow of a d.c. discharge (or when nitrogen is bombarded by past particles). In low frequency [2] and microwave discharges [3] there is evidence of indirect excitation; the best evidence of such processes comes from a study of the pink afterglow (P.A.) by BRÖMER and DÖBLER [4], who showed that the population rate of $N_2^+(B)$ is greater than the ionisation rate. Some plausible processes are:

$$N_2^+(X) + N_2^\dagger \rightarrow N_2^+(B) + N_2\,, \quad (1)$$

$$N_2^+(X) + e \rightarrow N_2^+(B) + e\,, \quad (2)$$

$$N_2^+(X) + N_2^m \rightarrow N_2^+(B) + N_2\,, \quad (3)$$

$$N + N_3^+ \rightarrow N_2^+(B) + N_2\,. \quad (4)$$

N_2^m, $N_2^\dagger$ represent metastable, electronically-excited and ground state, vibrationally excited N_2, respectively. The processes may well be complex; e. g. (1) may involve step-wise vibrational excitation of N_2^+ followed by collisional conversion between the X, A and B states.

* Present address: I.C.I. Fibres Ltd., Middlesbrough, Yorks.
** Request reprints etc. should be sent to Dr. B. BROCKLEHURST, Chemistry Department, The University, Sheffield S3 7HF, U.K.

Interconversion of nitrogen ions (N^+, N_2^+, N_3^+, N_4^+) does occur in nitrogen afterglows [5, 6] but there is no evidence that (4) leads to excitation of N_2^+; it appears to be ruled out by the absence of N_2^+ emission from an auxiliary discharge in the Lewis-Rayleigh afterglow [3]. The other three processes are less easily distinguished because of the case of exchange of energy between these species. For example, in afterglows, process (5) [7] leads to rapid equilibration between the energy distributions of $N_2^\dagger$ and electrons:

$$N_2^\dagger + e \rightleftharpoons N_2 + e\,, \quad (5)$$

i. e. (1) is not easily distinguished from (5) followed by (2).

The study [8] of electron beam excitation of nitrogen has therefore been extended to gas flowing from a microwave discharge: this is known to contain high concentrations of $N_2^\dagger$ [9]. Though still complicated, the excitation processes are likely to be simpler than in the discharge or the P.A.

"Oxygen-free" nitrgen (British Oxygen Gases) was used: ready production of the P.A. indicated adequate purity. Before reaching the electron-beam cell, the gas flowed through a straight silica tube, 10 mm i. d.; the position of the microwave cavity could be adjusted along this tube to give distances of 15 – 120 cm between it and the cell. Electrons accelerated to 50 keV *in vacuo* passed through a thin aluminum foil [8] into the nitrogen stream at right angles to the flow. Successful preliminary experiments were carried out in a pyrex cell similar to that used before [8]: it was a cylinder, 3 cm in diameter, the flowing gas entering and leaving through 1 cm diameter side tubes; however, the flow pattern in the cell was uncertain and the P.A. often appeared in the cell. Better results were obtained with a continuous flow tube with 1 cm diameter side arms carrying the electron beam: this reduced the beam current (maximum reached was 1.6 μA) and the luminescence was weak. Light emitted at right angles to both flow and beam was analysed with a Bausch and Lomb $f/4$ grating monochromator (33-86-02)

and an E.M.I. 9558Q photomultiplier. Corrections were made for scattered light from the discharge.

The microwave discharge produced the yellow Lewis-Rayleigh discharge downstream, but it did not interfere with measurements in the ultra-violet. The P.A. appeared over a distance of several cm, separated from the discharge by a dark space; the P.A. was much brighter than the beam luminescence. At the low pressures used, both first negative and second positive band systems were relatively strong in the electron beam; first positive was very weak [8]. Because of the low intensity, measurements were concentrated on the first negative $(0-0)$ band at 3914 Å and the neighbouring second positive bands. When the discharge was switched on, the latter were hardly affected, but the intensity of first negative increased: the enhancement is expressed as the ratio of intensities with and without the discharge. In a typical experiment, a pressure of 7 Torr and a measured linear flow-rate of 4.2 m s^{-1} were used (the actual flow rate must be greater when the discharge is on because of heating of the gas). The enhancement factor was 6 at 30 cm from the discharge (just downstream of the P.A.) and it fell steadily to 1.4 at 120 cm. The enhancement was greater at higher flow rates and with increasing pressure it increased to a maximum at 7 Torr and then decreased slowly. For example, at 25 Torr (no P.A. visible) enhancements of 4 and 2 occurred at 20 and 40 cm below the discharge respectively. The first negative intensity was proportional to the electron beam current between 0.2 and 1.6 μA.

In nitrogen at 7 Torr and 300 K, a 1 μA electron beam alone will produce ions at $\sim 2 \cdot 10^{13}$ cm^{-3} s^{-1}: 10% will be excited in the B state and only 15% of these will emit because of collisional deactivation [8]. An enhancement factor of 6 corresponds to a photon emission rate from the B state of $\sim 2 \cdot 10^{12}$ cm^{-3} s^{-1}; i. e. the intensity with the beam alone can be used to calculate the absolute yield. (Uncertainties due to the cell geometry are considerable but cancel when the luminescence rate is compared with the ionization rate.) To estimate the ion concentration, the rate of loss is needed: estimates for various processes (downstream flow, recombination etc.) suggest that the dominant loss process is ambipolar diffusion to the walls, especially when the discharge is on because of electron heating by (5). An estimate of ion and electron concentrations of $1-5 \times 10^8$ cm^{-3} appears reasonable (cf. 5×10^9 in the P.A. [10]). In addition to N_2^+, the discharge introduces nitrogen atoms and metastables: the density of the $N_2(A)$ state is $\sim 2-4 \times 10^9$ cm^{-3} [11]. A similar value for the a′ state can be calculated from its deactivation rate [6] if it is produced efficiently from N atom recombination: concentrations of other states should be smaller. The discharge will also raise the kinetic temperature, but this alone would cause a small reduction in the first negative intensity: at constant pressure, the density will decrease, and the excitation rate and collision rate will both fall, depending on T^{-1} and $T^{-\frac{1}{2}}$ respectively.

From the values above, process (3) would require a cross-section of $\sim 10^{-11}$ cm^2. The cross-section of (2) is known [12]: it would account for only 1% of the observed intensity even if all the electrons had sufficient energy: also the intensity would depend on the square of the beam current, contrary to observation. So (2) and (3) can be ruled out: they are probably not important in the P.A. either, but (2) will become significant at higher ion densities e. g. in some discharges. The plausibility of (1) has been discussed previously [3]. It accounts for the present observations: the effect of flow-rate and the initial increase with pressure are due to the loss of vibrating molecules to the tube walls. At higher pressures, production of vibrating molecules in the dicharge must become less efficient because of the higher mass flow-rate: the P.A. also appears, then disappears with increasing pressure.

In addition to demonstrating the occurrence of (1), the original aim of this work was to measure the rate constant of the process.

An order of magnitude estimate of 2×10^{-15} cm^{-3} s^{-1} can be made for the region just below the P.A.; this is reasonable if the vibrational temperature is $\geqq 3000$ K. In an attempt at measuring this temperature, a study of the heat content of the flowing gas was made, but no consistent interpretation was possible. This is probably due to the failure of the vibrational energy to follow a Boltzmann distribution under these conditions [13]: when the kinetic temperature falls well below the "vibrational temperature", an anharmonic oscillator will take up a distribution in which the population of higher levels will greatly exceed that expected by a logarithmic extrapolation from lower levels. Evidence for this redistribution as the gas cools between discharge and P.A. was found in these experiments: the "dark space" could be extended by working at high flow-rates: at 7 Torr and 15 m s^{-1}, an enhancement of 7 was observed 10 cm above the P.A. (15 cm below the discharge) and this *increased* to 15 at 2 cm above the P.A. In the "dark space", the Lewis-Rayleigh afterglow is weak, and it was possible to study the first positive bands: enhancement by the discharge was again observed and it increased as the P.A. was approached: this can also be ascribed to the redistribution, since the Franck-Condon factors for the transition, $B \leftarrow X$, favour excitation of the first positive bands in the visible from high vibrational levels. The electron beam excitation is not strong enough for detailed spectroscopic studies and the increasing enhancement of the first negatve bands in the dark space could be due to a decrease in the ion loss rate with increasing density. However, spectroscopic studies [14] with an auxiliary, radio-frequency discharge have demonstrated that the redistribution does occur in this region.

The authors thank Dr. DEMONCHY for communication of results before publication and the Science Research Council for a grant for equipment and for maintenance of one of them (R. J. A.).

[1] O. OLDENBERG, J. Opt. Soc. Amer. **61**, 1092, 1098 [1971].
[2] H. H. BRÖMER and F. SPIEWECK, Z. Phys. **184**, 481 [1965].
[3] B. BROCKLEHURST and R. M. DUCKWORTH, J. Phys. B **1**, 990 [1968].
[4] H. H. BRÖMER and F. DÖBLER, Z. Phys. **185**, 278 [1965].
[5] H. H. BRÖMER and J. HESSE, Z. Phys. **219**, 269 [1969].
[6] A. R. DEMONCHY, Thesis, University of Amsterdam 1970.
[7] I. R. HURLE, J. Chem. Phys. **41**, 3592 [1964].
[8] B. BROCKLEHURST and F. A. DOWNING, J. Chem. Phys. **46**, 2976 [1967].
[9] A. M. BASS, J. Chem. Phys. **40**, 695 [1964]. — Y. TANAKA, F. R. INNES, A. S. JURSA, and M. NAKAMURA, J. Chem. Phys. **42**, 1183 [1965].
[10] S.-L. CHEN and J. M. GOODINGS, J. Chem. Phys. **50**, 4335 [1969].
[11] J. A. MEYER, D. W. SETSER, and W. G. CLARK, J. Phys. Chem. **76**, 1 [1972].
[12] A. R. LEE and N. P. CARLETON, Phys. Lett. **27 A**, 195 [1968].
[13] B. BROCKLEHURST, Nature Phys. Sci. **236**, 12 [1972] and references therein.
[14] J. ANKETELL and B. BROCKLEHURST, unpublished work.

Low-temperature Heat Capacity and Paramagnetic Susceptibility Measurements on some Tetragonal Nickel(II) Compounds

F. W. KLAAIJSEN

Kamerlingh Onnes Laboratory, State University, Leiden
The Netherlands

J. REEDIJK * and H. T. WITTEVEEN

Gorlaeus Laboratory, State University, Leiden
The Netherlands

(Z. Naturforsch. **27 a**, 1532—1534 [1972]; received 8 September 1972)

Zero-field splittings have been determined for the spin triplet ground state of Ni(II) in Ni(pyrazole)$_4$Cl$_2$ and Ni(pyrazole)$_4$Br$_2$, by means of heat capacity measurements in the 1—80 K region and by paramagnetic susceptibility measurements in the 2—80 K region.

The results of both measurements can be fitted with theory using the spin Hamiltonian

$$H = g\beta H S + D[S_z^2 - S(S+1)/3] + E(S_x^2 - S_y^2)$$

with the parameter D equal to 7.2 cm^{-1} for the chloride and 5.4 cm^{-1} for the bromide. The value of E appeared to be close to zero for both compounds, indicating nearly axial symmetry.

The anisotropic g-values (calculated from the susceptibility) are $g_\perp = 2.21 \pm 0.03$ and $g_\parallel = 2.14$ for the chloride and $g_\perp = 2.20$, $g_\parallel = 2.12$ for the bromide.

Introduction

Nickel(II) ions ($3d^8$) with axially distorted octahedral coordination are known to yield a spin splitting of the ground state ($^3A_{2g}$), even in the absence of a magnetic field [1]. Usually these splittings are of the order of 0.1—1.0 cm^{-1} and are caused by second-order pin-orbit coupling. The magnitude of this splitting, D, deends upon the orbital splittings in the excited states (l. c. [1, 2]).

LIEHR and BALLHAUSEN [3] derived D from the orbital splittings by means of the relation $D = -9\,k\,\lambda^2/\Delta^2$, with k = the magnitude of the trigonal $^3T_{2g}$ splitting, λ = spin-orbit coupling constant and Δ = distance between the $^3A_{2g}$ and $^3T_{2g}$ term. In a previous study [4—6] on the spectra, structure and bonding of tetragonal pyrazole compounds, we found unusually large orbital splittings for a number of compounds Ni(ligand)$_4$(anion)$_2$. This would yield zero-field splitting much larger than 1 cm^{-1}, using the relation of LIEHR and BALLHAUSEN [3].

In order to examine if a relation exists between D. the orbital splitting and the nature of the ligand and the anion, we determined D-values for a number of compounds of formula NiL_4X_2, in which L is a pyrazole or imidazole ligand, and X is a halide or nitrate anion. The D-values were determined with the aid of specific heat and paramagnetic susceptibility measurements. The results for two typical examples are discussed in the present paper.

Experimental

Ni(pyrazole)$_4$Cl$_2$ and Ni(pyrazole)$_4$Br$_2$ were prepared from the metal salt hydrates by adding the ligand in the ratio 1 : 4 in ethanol as a solvent. The compounds were checked for purity by chemical analysis. The crystal structures of both compounds have been published [7, 8].

The heat capacity measurements were performed with the usual heat pulse method. To cool the sample to bath temperature a mechanical heat switch was used. The powdered salts were pressed into a thin walled gold-plated finned copper calorimeter to improve internal heat contact [9].

The paramagnetic susceptibility was measured by means of a PAR vibrating sample magnetometer, model 150, in the 2—80 K region at fields around 5000 Oersted.

Results and Discussion

From the methods avaialable for determining large D-values (viz. single-crystal EPR spectra, heat capacity measurements, single-crystal magnetic anisotropies, paramagnetic powder susceptibilities, and direct spectroscopic measurements), we have chosen the heat capacity and powder paramagnetic susceptibility at low temperatures, as single crystals of the compounds of sufficiently large size were not available and far-infrared and Raman spectra were expected to be disturbed by interaction with lattice vibrations.

* Reprint requests to Dr. J. REEDIJK, Department of Chemistry, State University, P.O. Box 75, Leyden, The Netherlands.

Figure 1 and 2 show the measured heat capacities in the 1 – 14 K region for the chloride and bromide respectively. The high temperature specific heat has been omitted from the figures for clearness. Both salts have an anomalous heat capacity in the He-temperature region. In order to substract the lattice heat capacity a $C T^2$ vs. T^5 plot was made. The estimated lattice heat capacities are drawn in the figures and can be represented by a three-dimensional Debye temperature, Θ_D, of 64.2 K for the chloride and 63.2 K for the bromide. The resulting heat capacity after subtraction of the lattice contribution is interpreted as a Schottky anomaly resulting from the Ni(II) ion, which has a low-lying singlet and a doublet at 7.2 cm^{-1} for the chloride and at 5.4 cm^{-1} for the bromide. The best theoretical Schottky heat capacity curves are drawn in the figures.

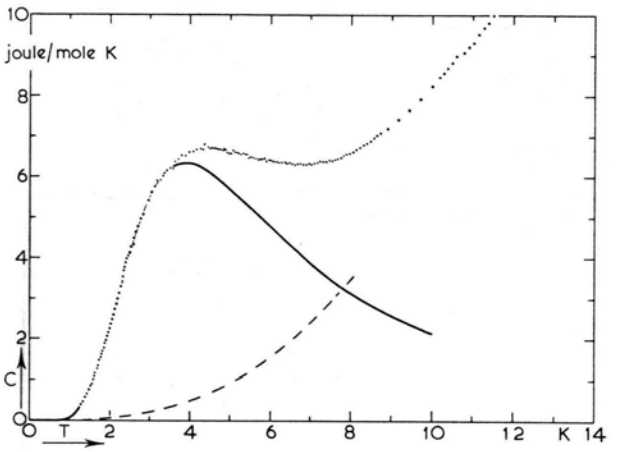

Fig. 1. C_p vs. T for $Ni(Pz)_4Cl_2$ (dotted curve). The dashed line is the estimated lattice heat capacity. The full curve is the theoretical Schottky heat capacity anomaly for $D=7.2\ cm^{-1}$.

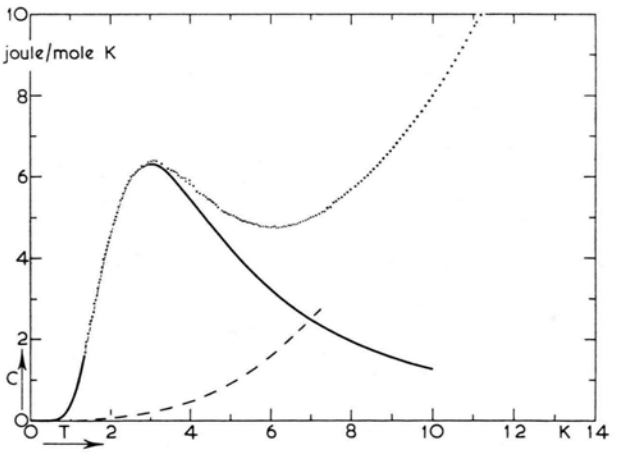

Fig. 2. C_p vs. T for $Ni(Pz)_4Br_2$ (dotted curve). The dashed line is the estimated lattice heat capacity. The full curve is the theoretical Schottky heat capacity anomaly for $D=5.4\ cm^{-1}$.

The observed magnetic susceptibility of the compounds was tried fitted with the theoretical expression for χ as a function of D, $g_{\parallel}$, $g_{\perp}$ and T. However, the usual theoretical expressions [10, 11] do not take into account the field dependent part of the susceptibility, and as our compounds were investigated at fields near 5000 Oersted, this would introduce serious errors.

Therefore we made use the basic equation for the susceptibility

$$\chi = N \Sigma (\partial w/\partial H)\ \exp\{-w/kT\}/H \Sigma \exp\{-w/kT\}$$

and calculated the *ab initio* χ values directly from this equation and the matrix for the $^3A_{2g}$ ground term under simultaneous zero-field splitting and magnetic field splitting (Table 1).

Table 1. Matrix of simultaneous action on $^3A_{2g}$ by zero-field splittings and magnetic fields.

M_S	−1	0	+1
−1	$D-g_{\parallel}\beta H_z$	$\sqrt{2}\, g_{\perp}\beta H_x/2$	0
0	$\sqrt{2}\, g_{\perp}\beta H_x/2$	0	$\sqrt{2}\, g_{\perp}\beta H_x/2$
+1	0	$\sqrt{2}\, g_{\perp}\beta H_x/2$	$D+g_{\parallel}\beta H_z$

The principal susceptibilities $\chi_{\parallel}$ and $\chi_{\perp}$ thus obtained, are averaged by the relation

$$\chi_{powder} = \tfrac{2}{3}\chi_{\perp} + \tfrac{1}{3}\chi_{\parallel}$$

and the observed χ vs. T is compared with several of these theoretical curves. First a rough value for D is obtained from extrapolation to $T \to 0$ of the expression [11]

$$\chi_{powder}(0) = 4N\beta^2 g_{\perp}^2/3D$$

with an initial value for $g_{\perp}$ obtained from the averaged value in the powdered compound at high temperature. Then the rough values were refined by fitting with the experimental curves. The splitting in the doublet was found to be very close to zero and is ignored in the fitting.

The results of the best fit of χ vs. T with D, $g_{\parallel}$, $g_{\perp}$ are listed in Table 2, together with the D and E values obtained from the heat capacity measurements. The ex-

Table 2. Zero-field parameters and g-values for compounds $Ni(pyrazole)_4X_2$.

Compounds	Heat capacity		Susceptibility		
	D (cm^{-1})	E (cm^{-1}) [a]	D (cm^{-1})	$g_{\parallel}$	$g_{\perp}$
$Ni(Pz)_4Cl_2$	7.2(1) [b]	0.0(1)	7.2(2)	2.14(3)	2.21(3)
$Ni(Pz)_4Br_2$	5.4(1)	0.0(2)	5.5(2)	2.12(3)	2.20(3)

[a] E stands for the doublet splitting.
[b] Uncertainties in the last digit are shown between parenthesis.

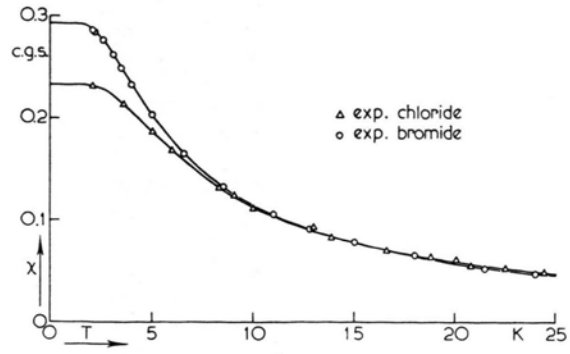

Fig. 3. χ vs. T for $Ni(Pz)_4X_2$ with X=Cl and Br. The calculated curves for the parameters listed in Table 1 are drawn through the experimental points.

perimental χ vs. T curves are depicted in Figure 3. As is seen from Table 2, the results of both measurements completely overlap, indicating the practical utility of these techniques to obtain zero-field parameters from powder data. The rather large uncertainties in the g-values (Table 2) are caused by weighting errors and by slight temperature dependence of the g-values.

The magnitude of the D-values in the present compounds is quite larger, but smaller and of opposite sign than predicted by LIEHR and BALLHAUSEN [3] from the orbital splittings [4].

We are extending these investigations to similar Ni(II) compounds with other anions and ligands and to calculations of D from the orbital splittings in the excited states, using second-order spin-orbit interactions.

[1] C. J. BALLHAUSEN, Introduction to Ligand Field Theory, McGraw-Hill, London 1962.
[2] J. REEDIJK and B. NIEUWENHUIJSE, Rec. Trav. Chim. **91**, 533 [1972].
[3] A. D. LIEHR and C. J. BALLHAUSEN, Ann. Phys. (New York) **2**, 134 [1959].
[4] J. REEDIJK, Rec. Trav. Chim. **89**, 993 [1970].
[5] R. D. DOWSING, B. NIEUWENHUIJSE, and J. REEDIJK, Inorg. Chim. Acta **5**, 301 [1971].
[6] J. REEDIJK, B. A. STORK-BLAISSE, and G. C. VERSCHOOR, Inorg. Chem. **10**, 2594 [1971].
[7] C. W. REIMANN, A. D. MIGHELL, and F. A. MAUER, Acta Cryst. **23**, 135 [1967].
[8] A. D. MIGHELL, C. W. REIMANN, and A. SANTORO, Acta Cryst. **B 25**, 595 [1969].
[9] F. W. KLAAIJSEN, to be published.
[10] T. WATANABE, J. Phys. Soc. Japan **17**, 1865 [1962].
[11] R. PRINS, J. D. W. VAN VOORST, and C. J. SCHINKEL, Chem. Phys. Letters **1**, 54 [1967].